A Platinum Open Access Journal for Organic Chemistry

Review

Free to Authors and Readers | DOAJ Seal | *Arkivoc* **2022**, part iii, 112-132

An overview on the role of cyclodextrins in the synthesis of silver nanoparticles by chemical reduction

Carla Gasbarri*and Guido Angelini

Department of Pharmacy, University "G. d'Annunzio" of Chieti-Pescara, via dei Vestini, 66100, Chieti, Italy
Email: carla.gasbarri@unich.it

Dedicated to Prof. György Keglevich on the occasion of his 65th birthday

Received 05-22-2022 **Accepted** 06-23-2022 **Published on line** 07-02-2022

Abstract

The association between cyclodextrins (CDs) and silver nanoparticles (AgNPs) has been successfully exploited in a large number of applications. Generally, CDs act as stabilizers, however, their reactivity as reducing agents can be directly involved in the synthesis of AgNPs. Herein, the most recent results regarding AgNPs prepared by chemical reduction from native α-, β- and γ-cyclodextrins are reported. The behavior of CDs in host-guest inclusion complexes onto the metal surface, and the effects on the AgNPs properties have also been examined. Unlike β-CD/AgNPs and γ-CD/AgNPs, additional reducing agents were required for the investigated α-CD/AgNPs.

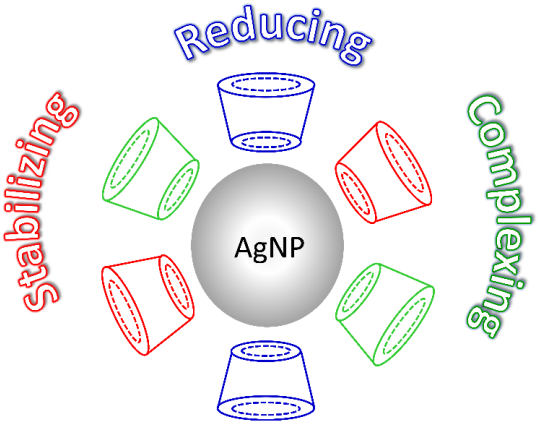

Keywords: Cyclodextrins, silver nanoparticles, inclusion complex, reduction.

Table of Contents

1. Introduction

The main advantage of the production of silver nanoparticles (AgNPs) consists of their great versatility due to both biological activities and chemical properties. As a result, medical devices, chemical sensors, cosmetics, optical and textile materials based on silver nanoparticles are still being developed and optimized.[1-8] The role of AgNPs as catalysts in organic reactions, and their effects on kinetic rate constants, are also becoming deeply investigated.[9-16]

It is well known that the synthesis of AgNPs can be performed by physical, chemical, and biological methods resulting in different sizes, shapes, and surface properties.[17-26] Recently, "green" approaches have been proposed using eco-friendly conditions[27] and reagents extracted from plants or agricultural waste.[28,29] Regardless of the adopted synthesis, the evidence of the formation of AgNPs in aqueous solution, and their characterization, are performed by means of specific instrumental methods and analysis.

UV-vis spectroscopy is one of the most commonly used techniques to demonstrate the presence of AgNPs in solution by means of the appearance of the typical surface plasmon resonance (SPR) band at approximately 400 nm. The SPR absorbance intensity is highly sensitive, and strictly connected to the yellowish color of the solution, while its position is affected by the surrounding environment of the metal surface. Furthermore, the SPR amplitude tends to reflect the shapes and dimensions of the nanoparticles: a narrow peak is generally associated with AgNPs which are spherical and uniform in size while blue or red shifting indicates the reduction or increase in the AgNPs dimensions, respectively.

Transmission electron microscopy (TEM) and field-emission scanning electron microscopy (FE-SEM) provide information about morphology, size, and dispersity of the nanoparticles, while Fourier-transform infrared spectroscopy (FT-IR) and surface-enhanced Raman scattering (SERS) spectroscopy highlight chemical interactions directly involving the metal surface.

Zeta potential analysis allows for measurement of the surface charge, which can be assumed to be a parameter used to predict the AgNPs stability in solution. High absolute surface charge suggests that repulsion between the nanoparticles occurs, limiting the aggregation process. Conversely, low absolute surface charge suggests that nanoparticles tend to associate over time.

Hydrodynamic diameter, polydispersity, and statistical particle distribution can be determined by dynamic light scattering. Finally, oxidation states of the metal and chemical valence states are obtained by X-ray photoelectron spectroscopy (XPS).[30-37]

Although the AgNPs possess large surface areas and high reactivity, capping agents are generally added as stabilizers during the synthesis to hamper the aggregation phenomena, avoid surface oxidation, and promote the interactions in the biological environment.[38-41] In many cases, however, modifications in the properties and functions of the final nanoparticles could be observed.[42]

The association between cyclodextrins and silver nanoparticles has successfully been exploited in several fields for different potential applications. Cyclodextrins are well known macrocyclic oligosaccharides composed of alfa-(1,4)-linked-D-glucopyranose units, forming truncated-cone structures of 0.78 nm in heighth.[43] The narrower side corresponds to the primary rim which exhibits the primary hydroxyl groups that are more flexible and involved in more extensive H-bonding than the secondary hydroxyl groups which are found in the wider side of the cyclodextrin cone corresponding to the secondary rim (Figure 1). [44]

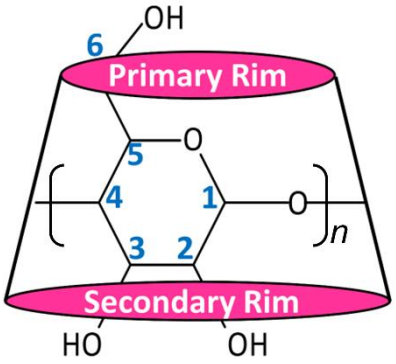

Figure 1. Structure of a native CD molecule (*n* = 6, 7, 8).

The coexistence of the hydrophobic inner cavity and hydrophilic external surface allows for the establishment of hydrophobic interactions, van der Waals forces, intermolecular hydrogen bonding with organic and inorganic species, and generate a large variety of host–guest inclusion complexes by increasing the solubility of highly lipophilic molecules having the tendency to aggregate.[45-53] Moreover, specific hydrophobic interactions within the CDs cavities were observed, even in the cases of aromatic hydrocarbons which were too large in size to be included as the guest.[54]

CDs are divided into alpha-cyclodextrin (α-CD), beta-cyclodextrin (β-CD), and gamma-cyclodextrin (γ-CD) depending on the presence of 6, 7 or 8 D-glucopyranose units in the structure, respectively. Among these, β-CDs represent the most employed cyclodextrin for clinical and food applications, especially due to its drug-loading capacity and inexpensiveness. Several derivatives are obtained by functionalization of the alcoholic groups to improve solubility, and reduce toxicity, in comparison to natural β-CD. Hydroxypropyl-β-cyclodextrin, methylated-β-cyclodextrin, and sulfobutylether-β-cyclodextrin are mentioned as relevant examples.[55-60]

The presence of native CDs during the synthesis of silver nanoparticles allows for the formation of shape-controlled AgNPs by limiting the nanoparticle growth after nucleation. Interestingly, after removal of the CDs, the electronic properties of the nanoparticles were unmodified.[61-64]

One silver nanoparticle is generally too large to be included into the hydrophobic cavity of the β-CD, however, interactions between the metal surface and the hydroxyl groups of the macrocycle can be established via chemisorption.[65] The chemical conjugation between cyclodextrins and nanoparticles through specific linkers allows the enhancement of the stability and solubility of AgNPs, and improves their antimicrobial activities and sensing properties such as fluorescence and absorbance.[66-68]

Cyclodextrins-capped silver nanoparticles (CDs/AgNPs) were synthesized in different conditions by using α-, β- and γ-CDs and their common derivatives. In this review, innovative contributions to the preparation and application of CDs/AgNPs from natural CDs, without additional reducing agents, are reported. Firstly,

supramolecular systems from β-CD and γ-CD are described, and then the use of α-CD in specific applications is examined.

2. General Synthesis of CDs/AgNPs by Chemical Reduction

One of the most common syntheses of AgNPs is based on the chemical reduction of metal ions, generally from an aqueous $AgNO_3$ solution using $NaBH_4$ or citrate. This method consists of a rapid and easy one-step reaction which allows a large number of nanoparticles to be obtained in solution. In the case of a fast reaction, very small nanoparticles in size could be generated due to the rapid growth of few metal nuclei. In the case of a slow reaction, aggregates of large dimensions could be formed. It was observed that the reactivity and concentration of the reducing agent strongly affect the antimicrobial activity of the obtained nanoparticles by influencing the size, shape, and particle distributions.[69,70]

In the presence of $NaBH_4$, formation of CDs/AgNPs spherical in shape, and monodispersed in solution, were observed.[71] In the presence of sodium citrate, enhanced antibacterial activity of capped nanoparticles was detected in comparison to uncapped ones.[72]

Two examples of the synthesis of silver nanoparticles from $AgNO_3$ using (**a**) $NaBH_4$ and (**b**) citric acid as reducing agents, and performed in the presence of native cyclodextrins as stabilizers, are compared. The position of the surface plasmon resonance (SPR) band in the UV-vis spectra, mean dimension, and particle-size distribution by TEM analysis of the obtained AgNPs are reported in Table 1.

Table 1. Comparison of the CDs/AgNPs by chemical reduction in the presence of $NaBH_4$ (**a**) and citric acid (**b**)

	Structural properties[43]		(**a**) Reduction by $NaBH_4$[73]		(**b**) Reduction by Citric Acid[74]	
CDs	Inner cavity (nm)	Outer diameter (nm)	SPR λ_{max} (nm)	TEM mean size / nm (particle distribution)	SPR λ_{max} (nm)	TEM mean size / nm (particle distribution)
α-CD	0.57	1.37	398	6-9 ± 2.2 (83%)	399	1-3.5 ± 1.5 (87.8%)
β-CD	0.78	1.53	396	3-10 ± 2.9 (85%)	403	0.5-3.5 ± 1.0 (96.9%)
γ-CD	0.95	1.69	400	3-7 ± 1.9 (83%)	406	1.5-4.5 ± 3.0 (95.6%)

The spectroscopic and TEM data for the AgNPs/CDs from $NaBH_4$ reduction are in good agreement with those from citric acid reduction.

Independently of the cyclodextrin used for preparation, the CDs/AgNPs from $NaBH_4$ reduction were stable for 1 year when stored in the dark at room temperature, as demonstrated by UV-vis spectra, surface-charge and Raman scattering measurements. Interestingly, in non-equilibrium conditions for hydrodynamic stress, differences in the cyclodextrin effects on the AgNPs size and morphology were highlighted as follow: α-CD was more capable of inducing the formation of smaller or less dense nanoparticles than β-CD due to its higher intrinsic solubility, while, in the presence of γ-CD, enhanced stability and dominance of Gibbs-Marangoni flow were pointed out. In addition, self-aggregation of γ-CDs/AgNPs into small clusters was observed by TEM.

Similarly, the AgNPs/CDs from citric acid reduction were stable under storage at room temperature for nearly 6 months. Crystalline, and face-centered cubic structures were observed. In particular, α- and γ-CDs showed the tendency to induce wider and narrower particle-size distributions, respectively. β-CDs promoted

the formation of small AgNPs in comparison to those obtained from α- and γ-CD. In other cases of the synthesis of AgNPs by reduction, different types of morphologies could correspond to different β-CD/Ag molar ratios.[75]

The reduction of $AgNO_3$ in the presence of CDs acting as both stabilizing and reducing agents was generally carried out in aqueous solution at pH ≥ 10 with stirring and heating, depending on the cyclodextrin structure. The clear yellowish color of the solution can be assumed to be the first evidence of formation of the AgNPs .

3. Beta-CDs/AgNPs

Much work based on β-CD employed as both reducing and stabilizing agent for the synthesis of capped silver nanoparticles has been reported.[76-78] Generally, the reactions were performed at alkaline pH in the absence of organic solvents. The reduction of the Ag^+ ions by hydroxyl groups of the β-CDs implies their oxidation into carboxylic groups which coat the metal surface, providing further stabilization of the nanoparticles.[79]

β-CD/AgNPs, easily prepared in aqueous solution according to the method reported by Han *et al.*,[80] were characterized in our laboratory. Briefly, 1 mM of $AgNO_3$ was added to a solution containing NaOH and β-CD in a 1:1 ratio. The mixture was left stirring overnight in the dark at room temperature. The clear, yellow-brown final solution revealed the presence of silver nanoparticles (Figure 1a). The narrow SPR band at 406 nm confirmed that uniform and spherically-shaped β-CD/AgNPs were formed (Figure 1b). Scattering measurements indicated a mean diameter of 34 nm and polydispersity index of 0.24 (Figure 1c). Zeta potential analysis provided a surface charge of -36 mV, suggesting high stability in solution (Figure 1d).

(a)

(b)

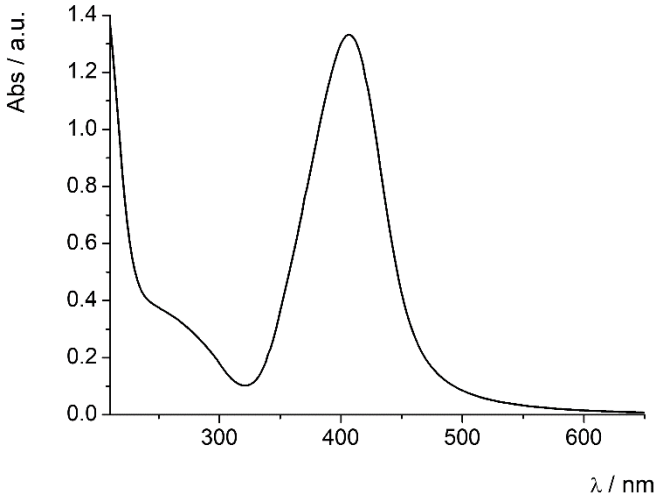

(c)

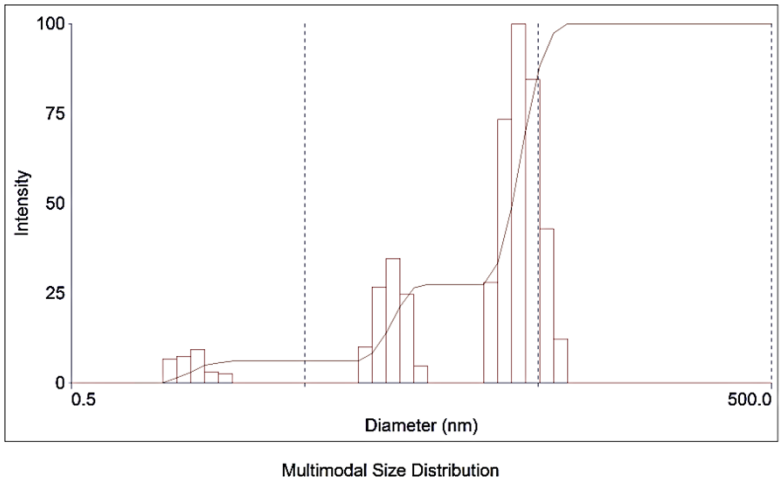

(d)

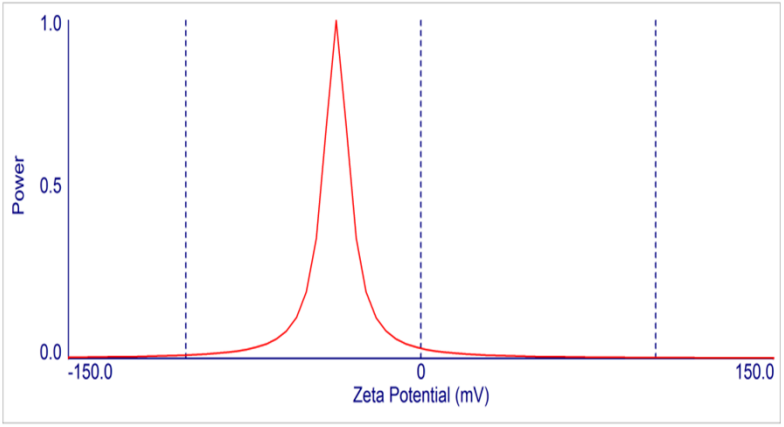

Figure 2. Characterization of the β-CDs/AgNPs: fresh prepared aqueous solution (**a**), UV-vis spectrum (**b**), scattering data (**c**) and zeta potential analysis (**d**).

Similar nanoparticles were recently prepared at neutral pH under eco-friendly conditions, using sulfobutylether-β-cyclodextrin as a reducing and stabilizing agent.[81]

The first synthesis of β-CD/AgNPs at room temperature was successfully reported by Premkumar and Geckeler.[82] The narrow SPR band at 414 nm in the UV-vis spectrum, the mean dimension of 34.5 nm in TEM images, and a single face-centered cubic phase of silver in XRD patterns represented the main properties of the aforementioned β-CD/AgNPs. Changing the concentration of the reagents (cyclodextrin, metal precursor and NaOH) or the reaction temperature resulted in the generation of nanoparticles having different size, shape, morphology, and distribution. Interestingly, an excess in cyclodextrin concentration leads to spherical, well-dispersed and small AgNPs, while lowering the cyclodextrin concentration tends to improve polydispersity by promoting agglomerates, as demonstrated by the red shift and the broadening of the SPR band.

The effects of NaOH concentration and the reaction temperature were also studied. In the former case, it was observed microscopically that the aggregation process occurs by decreasing the NaOH concentration from 40 to 5 mM. In the latter case, it was demonstrated that fast nucleation with the generation of small spherical particles occurs at 65° C, while aggregation of the small particles into short rod-like structures takes place at 4°C.

To establish the existence of interactions between the β-CD molecules and the metal surface in the investigated nanoparticles, the FT-IR spectra of the natural β-CD and β-CD/AgNPs were compared. Significant changes were reported in the intensities and positions of the peaks. The intensities associated with β-CD/AgNPs were strongly decreased in comparison to the data reported for pristine β-CD. Moreover, the appearance of the peak at 1384 cm^{-1}, due to the stretching of the carboxylate ions formed by oxidation of the hydroxyl groups during the reduction of Ag^{+} ions to Ag^{0}, and the strong high frequency shift of the –OH stretching band from 3391 to 3416 cm^{-1}, are in full agreement with the absorption of the β-CD molecules onto the nanoparticle. The FT-IR peak positions of the β-CD/AgNPs are reported in Table 2.

Table 2. Peaks in the FT-IR spectra of the β-CD/AgNPs

	FT-IR peak/cm^{-1}	
β-CD/AgNPs	1384, 1644	Stretching of the carboxylate ions
	946	α-1,4 linkage skeletal vibration
	759, 708, 574	ring vibration
	3416	–OH stretching band

Recently, some methods based on silver nanoparticles were developed for the detection of antibiotic residues in animal-derived food after treatment of veterinary diseases.[83-85] In particular, traces of norfloxacin in milk were identified through the inclusion of the drug into the β-CD cavity in β-CD/AgNPs previously obtained using β-CD as a reducing agent.[86] The formation of the norfloxacin/β-CD inclusion complex was demonstrated by theoretical and experimental analyses,[87] and its proximity to the nanoparticle surface induced relevant changes in the spectral properties of the β-CD/AgNPs. In the presence of norfloxacin, the surface plasmon resonance band of the β-CD/AgNPs solution shifts from 410 to 405 nm, and a decrease in the absorbance intensity can be observed. Moreover, a broad peak appears at 578 nm. Further evidence of the drug inclusion in the proximity of the metal surface was obtained by fluorescence spectroscopy. Fluorescence quenching is involved in several reactions under different conditions.[88,89] Generally, the formation of an inclusion complex tends to increase the intensity of the fluorophore encapsulated in the cyclodextrin cavity.[90] This trend can be observed for norfloxacin in the presence of different concentrations of β-CD. Interestingly, the quenching of the fluorescence of the investigated drug takes place in the presence of β-CD/AgNPs, suggesting that a short distance exists between the guest molecule and metal surface, according to the mechanism of Forster resonance energy transfer.[91] The fluorescence intensities emitted at 440 nm for the drug in its free form and in the presence of β-CDs and β-CDs/AgNPs are reported in Figure 3.

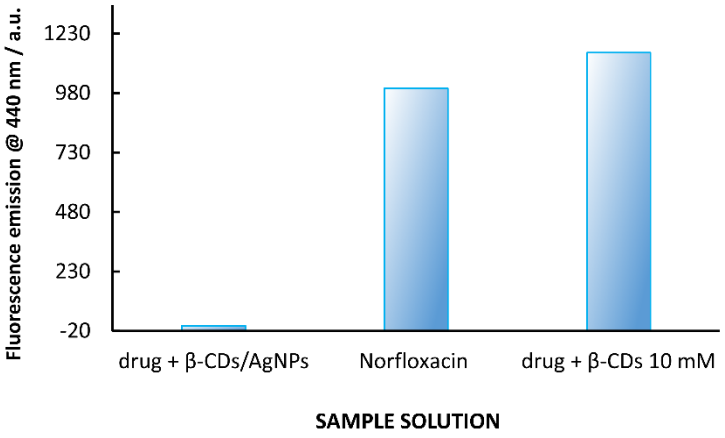

Figure 3. Comparison between the fluorescence emission intensity of norfloxacin in its free form and in the presence of β-CDs and β-CDs/AgNPs.

The effect of norfloxacin can be determined by measuring the surface potential charge and the mean diameter of the nanoparticles; the former changes from -26.7 to -12.65 mV, and the latter increases from 36.8 to 162.8 nm. The data suggested the presence of the inclusion complex from β-CD molecules involved in the AgNPs capping.

Other evidence for the detection of norfloxacin using β-CD/AgNPs was obtained from Raman spectroscopy. The typical peaks of the powder drug were observed for norfloxacin in a solution of β-CD/AgNPs, showing similar positions and intensities. In particular, the disappearance of the peaks at 852 cm^{-1} (due to the C-N vibrations), and at 923 cm^{-1} (due to C-H bending), indicated the formation of the inclusion complex of the drug with the β-CD cavity on the nanoparticle surface.[92] Conversely, the dominant peak at 1389 cm^{-1} from the ring-stretching vibration was found to be 17-fold higher than the corresponding peak observed in the spectrum of the AgNPs in the absence of cyclodextrins. A schematic illustration of the norfloxacin/β-CD inclusion complex adsorbed on the nanoparticle surface is presented in Figure 4.

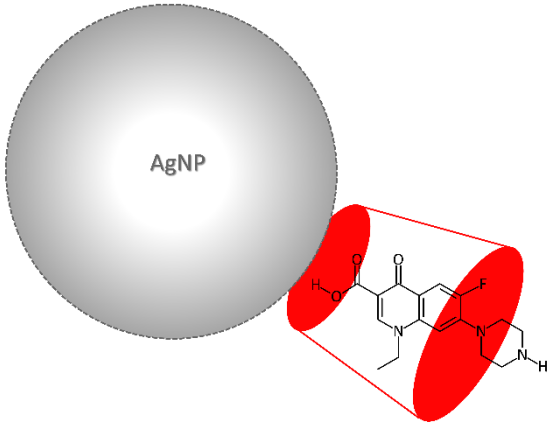

Figure 4. Schematic representation of the norfloxacin/β-CD capped AgNPs (not drawn to scale).

The advantages resulting from covering the AgNPs with β-CD could be enhanced by covalent interactions of the macrocyclic structure with the silver surface. Generally, molecules having a thiol group allow covalent bonding with the metal.[93,94] This functionalization prevents particle growth and aggregation. Recently, mono-

(6-mercapto-6-deoxy)-β-cyclodextrin was added to a β-CD/Ag solution with stirring to yield the final β-CD-S-AgNPs.[95] The shifting from 420 to 402 nm observed in the UV-vis spectra suggests that the covalently functionalized nanoparticles are smaller in size in comparison to the β-CD/AgNPs, according to TEM analysis. The investigated nanoparticles can be used as sensitive surface-enhanced Raman scattering (SERS) substrates for the recognition of specific drugs, such as Losartan and Prazosin. Although molecules having small size could be incorporated into the CD cavity in the place of the specific analyte, the method based on β-CD-S-AgNPs seems to limit the problem of the weak signal associated with the SERS electromagnetic mechanism.[37,96.]

An innovative and eco-friendly approach to obtaining AgNPs from CDs consists of applying synergistic effects, in which both host and guest act as reducing agents, into to the inclusion complex. Curcumin (CUR), the polyphenol responsible for the typical yellow color of turmeric, was previously employed as both capping and reducing agent in the synthesis of AgNPs, however, organic solvents or chemical reagents were often required to overcome the low solubility of the CUR molecules[97-99]. The association with cyclodextrin offers the advantages of enhancing the anti-inflammatory, antimicrobial, and antioxidant properties of curcumin in solution, in the absence of potentially toxic chemical mediators. The CUR:β-CD inclusion complex exhibits 1:1 and 1:2 stoichiometries according to the changes in the ^{1}H-NMR spectra of β-cyclodextrin after the insertion of the guest. In particular, the chemical shifts of the internal protons of the β-cyclodextrin molecule H-3 from 3.643 to 3.790 ppm and H-5 from 3.606 to 3.679 ppm in addition to the disappearance of specific peaks related to curcumin between 6.50 and 7.60 ppm, clearly indicated the inclusion of the aromatic rings into the β-CD cavity.[100]

Recently, CUR was inserted into the cavity of hydroxypropyl-β-CD (HPβ-CD), and the complex obtained was added to silver nitrate in aqueous solution with boiling and stirring of the mixture for 3 h in the dark.[101] The yellow-brown color of the final solution confirmed the formation of CUR-Hβ-CD-capped AgNPs. TEM images showed structures which were spherically shaped with a mean size of about 42 nm. Dynamic Light Scattering (DLS) analysis indicated a hydrodynamic diameter of around 182 nm, and a polydispersity index of 0.196 was in agreement with a uniform distribution of nanoparticles. Zeta potential measurements suggested a high stability in solution due to the surface charge of -20 mV. All of these results seemed to indicate a distribution of CUR-HP-β-CD as a surrounding layer on the silver surface, in agreement with the data from AgNPs synthesized by reduction in the presence of curcumin.[97,102,103]

The CUR-HP-β-CD-capped AgNPs were loaded into bacterial cellulose hydrogel and tested for their antimicrobial and antioxidant properties. The broad spectrum antimicrobial activity shown against common wound infections, and the high cytocompatibility observed for the investigated hydrogels, demonstrated their potential use in wound-dressing applications.

4. Gamma-CDs/AgNPs

Generally, γ-CD/AgNPs were prepared by mixing γ-CD and $AgNO_3$ in aqueous solution, in the presence of NaOH (to reach a final pH ≥ 10) with stirring and heating up to 60-80 °C. The schematic synthesis of γ-CD-capped silver nanoparticles by chemical reduction is depicted in Figure 5.

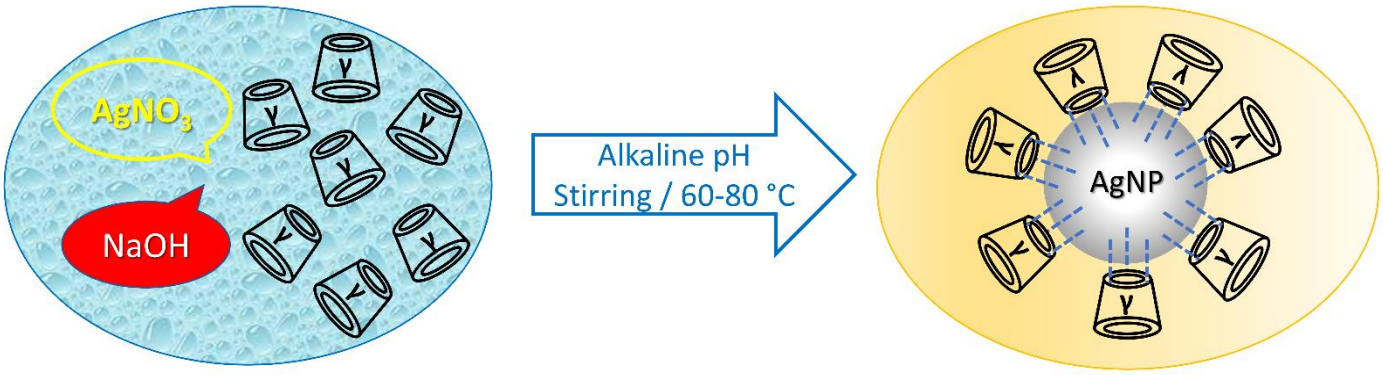

Figure 5. Schematic illustration of the synthesis of γ-CD-capped AgNPs by reduction (not drawn to scale).

Recently, γ-CD-capped silver nanoparticles were investigated as nanoprobes for the detection of pesticides [104] The nanoparticles afford high stability for at least 3 months under storage in the dark. Analogous capped Au nanoparticles were also synthesized. The narrow surface plasmon band at 417 nm and mean diameter of 20 nm observed by TEM and Atomic Force Microscopy (AFM) analyses indicated the presence of monodispersed and spherically-shaped nanoparticles in solution. In addition, their zeta potential value of -38 mV suggests that electrostatic repulsions between the surfaces hamper the aggregation process. The binding between the γ-CDs/AgNPs and chlorpyrifos (*O*,*O*-diethyl-O-[3,5,6-trichloro-2-pyridin-2-yl]-phosphorothioate) was studied to develop a detection method for pesticides in fruits and vegetables. It was observed that increasing the concentration of chlorpyrifos causes the SPR band of the γ-CDs/AgNPs to gradually decrease, while a broad shoulder appears between 450 and 700 nm due to the adsorption of the pesticide onto the nanoparticle surface. Increasing the adsorbate-concentration aggregation occurs by changing the size and shape of the nanoparticles, as indicated by the red shift in the UV-vis spectra, and the gradual change in the color of the solution from yellow to orange to deep green. Finally, the structural and vibrational changes induced in the Raman spectra suggest the deposition of mono- or multilayers of chlorpyrifos on the metal surface. These results are in good agreement with those reported for the silver nanoparticles decorated with the inclusion complex formed by γ-CDs and 1,5-dihydroxynaphthalene. The obtained nanoparticles were tested as fluorescent probes for dual-metal ions.[105] The affinity of the γ-CD rim for the silver surface was confirmed by the presence of the -OH stretching vibration displaced at 3443 cm^{-1} in the FT-IR spectrum. The SPR band at about 410 nm, and the TEM images, indicated the existence of spherical nanoparticles. Moreover, the 3d splitting doublet of 5.89 eV in the X-ray Photoelectron Spectroscopy (XPS) spectrum demonstrates that Ag is in its metallic state and supports the presence of γ-CD and silver in the composite.[106] The binding constant between the γ-CDs/AgNPs and the fluorescent guest 1,5-dihydroxynaphthalene was determined spectroscopically by the Benesi-Hildebrand equation.[107]

Spherical and polyhedral γ-CD/AgNPs can be prepared according to the method described by Premkumara and Geckeler for the β-CD-capped AgNPs, and applied in a ternary system for the molecular recognition and antibacterial activity of chloramphenicol.[108] The yellowish-brown solution of the γ-CD/AgNPs was obtained after reaction at 30° C with stirring for 24 h. The SPR band centered at 412 nm, the diameter in the range 20-30 nm, and the surface charge value of -30.1 mV were determined by UV-vis, TEM spectroscopy and zeta potential analysis, respectively.

FT-IR spectroscopy was carried out to confirm the capping of CDs on the metal surface. In particular, the peak at 1638 cm^{-1} was assigned to the stretching vibrations of carboxylate groups from the oxidation of the primary hydroxyl groups of the CDs to carboxylic acid during the reduction of Ag+ into Ag^0 in the synthesis of the nanoparticles. The dominant peak at 1414 cm^{-1} in the Raman spectra was also assigned to the symmetric

stretching vibration of the carboxylate functional groups.[82,109] Moreover, the high intensity of this peak and presence of elemental silver carbon and oxygen in the EDX pattern could provide further evidence of cyclodextrins anchoring onto the AgNPs surface.[109] It was observed that the inclusion of chloramphenicol into the obtained γ-CD/AgNPs creates a synergic antibacterial effect. Changes in the Raman signals confirmed that the encapsulation of the drug into the γ-CD cavity involves the nanoparticle surface.[110] The slight variations in the zeta potential value, and hydrodynamic size measured by dynamic light scattering in the presence and absence of chloramphenicol suggests that nanoparticle stability was independent of the drug loading.

5. Alfa-CDs/AgNPs

To the best of our knowledge, the use of α-CD as a stabilizing agent in the synthesis of silver nanoparticles by chemical reduction is limited, and the addition of an external reducing agent is needed to carry out the reaction. A green solution containing spherical, and relatively monodispersed α-CD/AgNPs having a SPR band at 382 nm was obtained from an aqueous solution of α-CD and $AgNO_3$ in the presence of $NaBH_4$ with stirring at room temperature.[111] XRD patterns pointed out the formation of a single face-centered cubic-phase silver metal. TEM analysis highlighted the tendency of the nanoparticles for self-assembly into 1-D pearl-necklace aggregates in a 1/10 diluted solution. This behavior was attributed to the generation of hydrogen bonds between the secondary faces of the α-CD and the surface of neighboring nanoparticles, by assuming an interparticle distance of about 5 nm. A schematic illustration of the surface interaction between closed nanoparticles is presented in Figure 6. It was also calculated that a single nanoparticle of about 5 nm can be covered by a layer of forty-four α-CD molecules. In concentrated colloids, the steric repulsions due to the proximity of the α-CDs were overcome, and complex networks formed from multiple interactions between the nanoparticles were observed.

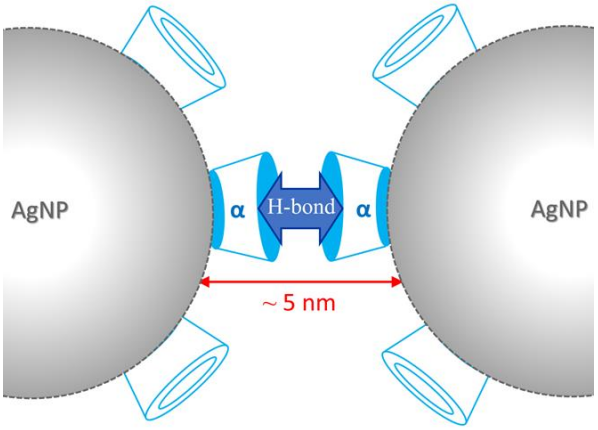

Figure 6. Schematic representation of the rim-rim interactions between α-CDs on the silver surface (not drawn to scale).

The adsorption of α-CDs on the AgNPs surface, and the capability to generate inclusion complexes with the aminoglycoside antibiotic spectinomycin (SPT), were recently proposed.[112] The α-CD/AgNPs were prepared using sodium citrate as a reducing agent with heating at 120° C, and then coated with bovine serum albumin by electrostatic interaction. The resulting yellow-green solution was composed of spherically-shaped, well-dispersed nanoparticles with a mean diameter of 62 nm and SPR band at 425 nm, as observed by TEM images

and UV-vis spectrum, respectively. The interactions between the SPT molecules and the cavity of α-CD on the albumin-coated nanoparticles induced vibrational and rotational changes in the FT-IR spectra in which the peaks at 1076, 1145, 1394, 1462 and 1648 cm^{-1} were shifted to 1091, 1161, 1408, 1475 and 1653 cm^{-1}, respectively. Moreover, the presence of the drug included in the host-guest complex or covalently bound to the metal induced strong enhancements of Raman signals by chemical and electromagnetic mechanisms.[96,113] Peaks at 485, 1447, 1128, 1224, 1320, 1578 cm^{-1} (due to ring breathing, C-N stretching, H-C-H deformation, and N-H bending vibrations, respectively) were observed in the SERS spectrum of SPT in a solution of nanoparticles. The quantitative analysis for detecting residual SPT traces in lamb and beef from treating bacterial infections, based on the albumin-covered α-CD/AgNPs, was performed by monitoring the large peak area at 485 cm^{-1} in the Raman spectra. It was observed that the amount of adsorbed SPT, the mixing time with the drug, and the nanoparticle aggregation degree could be taken into account to obtain the best performances.

The high affinity between α-CDs and nanoparticles was also observed in the case of AgNPs immobilized in thermo-sensitive hydrogels prepared by copolymerization of *N*-isopropyl acrylamide and 2-acrylamido-2-methyl-1-propanesulfonic acid, with *N*,*N*′-ethylenebis(acrylamide) acting as the cross-linker.[114] The silver nanoparticles were synthesized by adding pre-weighed hydrogels in $AgNO_3$ solution using $NaBH_4$ as a reducing agent. The changing of the hydrogel from colorless to black indicated the loading of AgNPs in the networks. The mean size of 3.5 nm and a silver concentration of 1.6% (wt) were determined by TEM analysis, and inductively-coupled-plasma atomic-emission spectrometry (ICP-AES), respectively. The catalytic effect of the system obtained was tested in the reduction of 4-nitrophenol to 4-aminophenol in aqueous solution. It was observed that the addition of α-cyclodextrin decreases the activation energy of the reaction and enhances the reduction rate. This synergistic-effect result was attributed to the inclusion complex formed by 4-nitrophenol and α-CD on the AgNPs surface of the hydrogel.

Innovative supramolecular systems based on α-CD as a porous liquid and chiral AgNPs were combined with planar conjugated molecules to investigate the chirality-induction mechanism.[115] The α-CD was prepared as a liquid with permanent microporosity (α-CDPL) according to the procedure reported by Wang *et al*.,[116] and mixed with silver nitrate in aqueous solution with stirring at room temperature. Sodium borohydride was then added with stirring for 10 min. The final solution of the α-CDPL-capped AgNPs (α-CDPL/AgNPs) showed a surface plasmon resonance band at around 400 nm in the UV-vis spectrum, and crystal planes of face-centered cubic phase of silver in the XRD pattern with mean size of about 168 nm in light scattering measurements. The anchoring of the α-CDPL molecules to the metal surface occurs by involving the hydroxyl groups and the carbonylic units as demonstrated by the shifts in the FT-IR spectra of α-CDPL/AgNPs.[117,118]

Analogously, β-CDPL/AgNPs and γ-CDPL/AgNPs were synthesized using β- and γ-CD porous liquids and characterized. All of the investigated CDPL/AgNPs were optically active.[116] An important goal was indeed reached for α-CDPL in the presence of the supramolecular system composed of AgNPs modified with 4-aminoazobenzene and L-cysteine. First, the silver surface was functionalized with L-cysteine according to the chemical reduction method.[119] The subsequent reaction between the amino units of the azobenzene molecules and the carboxylic groups of cysteine resulted in chiral silver nanoparticles having pH-dependent surface charges (Azo/AgNPs). The surface plasmonic band at 386 nm and a positive band at approximately 400 nm can be observed in the UV-vis and circular dichroism spectra, respectively. The presence of the azophenyl moiety on the metal surface was determined spectroscopically. In particular, the appearance of the C=C vibration peak at 1482 cm^{-1}, and the changes of the area of the vibration peaks at 1618 and 1384 cm^{-1}, were due to the introduction of the azobenzene derivative into the L-cys-modified AgNPs. Moreover, it was determined from the integral area ratio between the peaks at 7.91 and 3.38 ppm in the ^{1}H-NMR spectra that about 22% of the

carboxyl groups of the L-cysteine anchored on the nanoparticle surface reacted with the 4-aminoazobenzene molecules.

The hydrodynamic size and surface charge of Azo/AgNPs in solution were measured in the pH range 3-10. At pH values ≤ 7.5, aggregation was promoted, and positive zeta potential values could be determined due to the dominant cationic form of the amino groups. At pH values > 7.5, the dissociation of the carboxylic units into carboxylate anions takes place, and the nanoparticle surface becomes negatively charged.

In the presence of α-CDPL, the formation of the inclusion complex involving the azophenyl moieties of the chiral Azo/AgNPs occurs, as confirmed by the chemical shifts of the H-3 and H-5 protons of the α-CDPL in the ^{1}H-NMR spectra moving from 3.89 ppm and 3.73 ppm to 3.90 ppm and 3.74 ppm, respectively. Moreover, the chemical shifts of the 3-, 5-, and 10-H of the azobenzene structure changed after its insertion into the α-CDPL cavity based on a 1:1 stoichiometry (Figure 7).

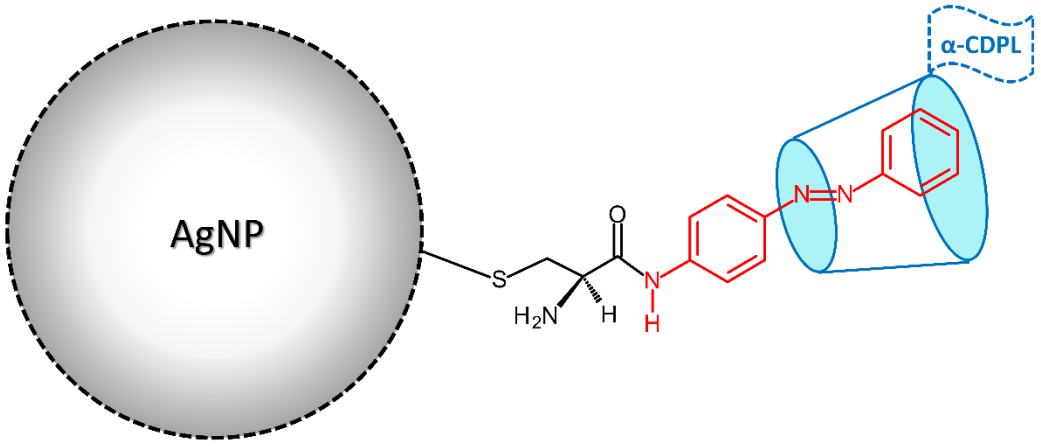

Figure 7. Schematic representation of the supramolecular system composed of Azo/AgNPs and α-CDs (not drawn to scale).

The chiral-induction ability of the investigated nanoparticles was tested using methylene blue and indigo carmine as probes. The sizes of the two planar molecules are too large to compete with azobenzene for the cyclodextrin cavity. It was observed that strong host-guest interactions between α-CDPL and azobenzene units on the silver surface enhanced the chirality of the Azo/AgNPs and the entire supramolecular system induced chirality of the planar probes. The adsorption of methylene blue and indigo carmine on the nanoparticle surface and their aggregation into twisted structures can be observed.[120] Furthermore, it was demonstrated that the chiral environment of the supramolecular system can be fine-tuned by changing the pH of the solution.

6. Conclusions

The presence of α-, β-, and γ-cyclodextrins during the synthesis of silver nanoparticles offers surface protection by covering the metal nanoparticles. Chemical reduction of the Ag^{+} ions by hydroxyl groups of the cyclodextrin rims offers the advantage of avoiding reducing agents, and provides further protection in covering the nanoparticles due to the CD carboxylic groups formed by oxidation. Different techniques can be employed to characterize the final nanoparticles, highlighting the existence of interactions between the CD molecules and

the metal surface. The formation of host-guest inclusion complexes in the proximity of the AgNPs could also be successfully applied to molecular and ion recognition.

The role of cyclodextrins as stabilizing, reducing and complexing agents allows the modulation of the AgNPs properties, leading to efficient, synergistic, and versatile systems for innovative applications in different fields. To the best of our knowledge, only in the case of α-CD is the presence of an additional reducing agent required to synthetize CDs/AgNPs. The versatility of α-CD was demonstrated in innovative supramolecular systems based upon chiral AgNPs.

References

1. Nair, L. S.; Laurencin, C. T. *J. Biomed. Nanotechnology* **2007**, *3* (4), 301-316. https://doi.org/10.1166/jbn.2007.041
2. Kelly, K.L.; Coronado, E.; Zhao, L.L.; Schatz, G.C. *J. Phys. Chem. B* **2003**, *107*, 668–677. https://doi.org/10.1021/jp026731y
3. Krutyakov, Y.A.; Kudrinskiy, A.A.; Olenin, A.Y.; Lisichkin, G.V. *Russ. Chem. Rev.* **2008**, *77*, 233–257. https://doi.org/10.1070/RC2008v077n03ABEH003751
4. Salata O. *J. Nanobiotechnology* **2004**, *2* (1), 3. https://doi.org/10.1186/1477-3155-2-3
5. Ahonen, P.; Schiffrin, D.J.; Paprotny, J.; Kontturi, K. *Phys. Chem. Chem. Phys.* **2007**, *9*, 651–658. https://doi.org/10.1039/B615309G
6. Choi, B.; Lee, H.H.; Jin, S.; Chun, S.; Kim, S.H. *Nanotechnology* **2007**, *18* (7), 075706. https://doi.org/10.1088/0957-4484/18/7/075706
7. Pisár, M.; Lukáč, M.; Jampílek, J.; Bilka, F.; Bilková, A.; Pašková, L.; Devínsky, F.; Horáková, R.; Opravil, T. *J. Mol. Liquids* **2018**, *272*, 60–72. https://doi.org/10.1016/j.molliq.2018.09.042
8. Gasbarri, C.; Ruggieri, F.; Foschi, M.; Aceto, A.; Scotti, L.; Angelini, G. *ChemistrySelect* **2019**, *4*, 9501–9504. https://doi.org/10.1002/slct.201902336
9. Li, A.Y.; Gellé, A.; Segalla, A.; Moores, A. Silver Nanoparticles in Organic Transformations in Silver Catalysis in Organic Synthesis, 723-793 chapt.12 First Edition. Edited by Chao-Jun Li and Xihe Bi. Published 2019 by Wiley-VCH Verlag GmbH & Co. KGaA. https://doi.org/10.1002/9783527342822.CH12
10. Ardakani, L.S.; Surendar, A.; Thangavelu, L.; Mandal, T., *Synthetic Comm.* **2021**, *51*(10), 1516-1536. https://doi.org/10.1080/00397911.2021.1894450
11. Angelini, G.; Pasc, A.; Gasbarri, C., *Colloids Surf. A* **2020**, *603*, 125235. https://doi.org/10.1016/j.colsurfa.2020.125235
12. Arya, G.; Kumari, R.M.; Sharma, N.; Gupta, N.; Kumar, A.; Chatterjee, S.; Nimesh, S., *J. Photochem. Photobiol. B: Biology* 2019, *190*, 50-58. https://doi.org/10.1016/j.jphotobiol.2018.11.005
13. Sheng, W.; Yang, Q.; Weng, J. *Curr. Org. Chem.* **2011**, *15*, 3692-3705. https://doi.org/10.2174/138527211797884638
14. Angelini, G.; Gansmüller, A.; Pecourneau, J.; Gasbarri, C., *J. Mol. Liquids* **2021**, *333*, 116000. https://doi.org/10.1016/j.molliq.2021.116000

15. Ghosh, S.; Suvra Khan, T.; Ghosh, A.; Chowdhury, A.H.; Haider, M.A.; Khan, A.; Manirul Islam Sk. *ACS Sustainable Chem. Eng.* **2020**, *8*, 5495−5513. https://doi.org/10.1021/acssuschemeng.9b06704
16. Angelini, G.; Scotti, L.; Aceto, A.; Gasbarri, C., *J. Mol. Liquids* **2019**, *284*, 592– 598. https://doi.org/10.1016/j.molliq.2019.04.048
17. Mafuné, F.; Kohno, J.Y.; Takeda, Y.; Kondow, T.; Sawabe, H. *J. Phys. Chem. B* **2000**, *104*, 9111-9117. https://doi.org/10.1021/jp001336y
18. Harra, J.; Makitalo, J.; Siikanen, R.; Virkki, M.; Genty, G.; Kobayashi, T.; Kauranen, M.; Makela, J.M. *J. Nanopart. Res.* **2012**, *14*, 870. https://doi.org/10.1007/s11051-012-0870-0
19. Abid, J.P.; Wark, A.W.; Brevet, P.F.; Girault, H.H. *Chem. Commun.* **2002**, 792-793. https://doi.org/10.1039/B200272H
20. Long, D.W.; Wu, G. Z.; Chen, S. M. *Phys. Chem.* **2007**, *76*, 1126–31.
21. Leopold, N.; Lendl, B. *J. Phys. Chem. B* **2003**, *107*, 5723–5727. https://doi.org/10.1021/jp027460u
22. Nasretdinova, G.R.; Fazleeva, R.R.; Mukhitova, R.K.; Nizameev, I.R.; Kadirov, M.K.; Ziganshina, A.Y.; Yanilkin, V.V. *Electrochem. Comm.* **2015**, *50*, 69-72. https://doi.org/10.1016/j.elecom.2014.11.016
23. Naganthran, A.; Verasoundarapandian, G.; Khalid, F.E.; Masarudin, M. J.; Zulkharnain, A.; Nawawi, N. M.; Karim, M.; Abdullah, C.A.C.; Ahmad, S.A. *Materials* **2022**, *15*, 427. https://doi.org/10.3390/ma15020427
24. Sun, Y.; Xia, Y. *Science* **2002**, *298*, 2176–2179. https://doi.org/10.1126/science.1077229
25. Tsuji, T.; Iryo, K.; Watanabe, N.; Tsuji, M. *Appl. Surf. Sci.* **2002**, *202*, 80–85. https://doi.org/10.1016/S0169-4332(02)00936-4
26. Scotti, L.; Angelini, G.; Gasbarri, C.; Bucciarelli, T. *Mater. Res. Express* **2017**, *4*, 105001. https://doi.org/10.1088/2053-1591/aa8c39
27. Raveendran, P.; Fu, J.; Wallen, S.L. *J. Am. Chem. Soc.* **2003**, *125*, 13940–13941. https://doi.org/10.1021/ja029267j
28. Lyu, Y.; Yu, M.; Liu, Q.; Zhang, Q.; Liu, Z.; Tian, Y.; Li, D.; Changdao, M.; *Carbohydr. Polym.* **2020**, *230*, 115573. https://doi.org/10.1016/j.carbpol.2019.115573
29. Sharma, V.K.; Yngard, R.A.; Lin, Y. *Adv. Colloid Interface Sci.* **2009**, *145*, 83–96. https://doi.org/10.1016/j.cis.2008.09.002
30. Jain, P.K.; Huang, X.H.; EI-Sayed, I.H.; EI-Sayed M.A. *Plasmonics* **2007**, *2*, 107-118. https://doi.org/10.1007/s11468-007-9031-1
31. Cobley, C.M.; Skrabalak, S.E.; Campbell, D.J.; Xia Y. *Plasmonics* **2009**, *4*, 171-179. https://doi.org/10.1007/s11468-009-9088-0
32. Xia, Y.; Tang, Z. *Chem. Comm.* **2012**, *48*, 6320–6336. https://doi.org/10.1039/C2CC31354E
33. Saeb, A.T.M.; Alshammari, A.S.; Al-Brahim, H.; Al-Rubeaan, K.A. *Sci. World J.* **2014**, 704708. https://doi.org/10.1155/2014/704708
34. Hammond, J.S.; Gaarenstroom, S.W.; Winograd, N. *Anal. Chem.* **1975**, *47*, 2193–2199. https://doi.org/10.1021/ac60363a019

35. Zhang, Z.; Shao, C.; Sun, Y.; Mu, J.; Zhang, M.; Zhang, P.; Guo, Z.; Liang, P.; Wang, C., Liu, Y. *J. Mater. Chem.* **2012**, *22*, 1387–1395. https://doi.org/10.1039/C1JM13421C
36. Singh, A.K.; Khan, F.S.T.; Rath, S.P. *Angew. Chem. Int. Ed.* **2017**, *56*, 8849–8854. https://doi.org/10.1002/anie.201705108
37. Centeno, S.P.; Lopez-Tocon, I.; Arenas, J.F.; Soto, J.; Otero, J.C. *J. Phys. Chem. B* **2006**, *110*, 14916-14922. https://doi.org/10.1021/jp0621373
38. Murphy, A.; Galon, R.; Jaiswal, A.K.; Jaiswal, S. *J. Food Chem. Nanotechnology* **2020**, *6* (4), 189-196. https://doi.org/10.17756/jfcn.2020-0101
39. Pencheva, D.; Bryaskova, R.; Kantardjiev, T. *Mater. Sci. Eng. C.* **2012**, *32*, 2048-2051. https://doi.org/10.1016/j.msec.2012.05.016
40. Hedberg, J.; Lundin, M.; Lowe, T.; Blomberg, E.; Wold, S.; Wallinder, I.O. *J. Colloid Interface Sci.* 2012, 369, 193-201. https://doi.org/10.1016/j.jcis.2011.12.004
41. Kvitek, L.; Panacek, A.; Soukupova, J.; Kolar, M.; Vecerova, R.; Prucek, R.; Holecova, M.; Zboril, R. *J. Phys. Chem. C* **2008**, *112*, 5825–5834. https://doi.org/10.1021/jp711616v
42. Duran, N.; Silveira, C. P.; Duran, M.; Martinez, D. S. T. *J. Nanobiotechnol.* **2015**, *13*, 55. https://doi.org/10.1186/s12951-015-0114-4
43. Szejtli, J. Cyclodextrin Technology; Kluwer Academic Publisher: Dordrecht, Springer Ed. 1988; https://doi.org/10.1007/978-94-015-7797-7
44. Szejtli, J. Past, *Pure Appl. Chem.* **2004**, *76* (10), 1825-1845. https://doi.org/10.1351/pac200476101825
45. Ji, X.; Ahmed, M.; Long, L.; Khashab, N.M.; Huang, F.; Sessler, J.L. *Chem. Soc. Rev.* **2019**, *48*, 2682–2697. https://doi.org/10.1039/C8CS00955D
46. Zhang, Y.M.; Liu, Y.H.; Liu, Y. *Adv. Mater.* **2020**, *32*, 1806158. https://doi.org/10.1002/adma.201806158
47. Uekama, K.; Hirayama, F.; Irie, T. *Chemical Rev.* **1998**, *5*, 2045–2076. https://doi.org/10.1002/CHIN.199839330
48. Marques, H.M.C. *Flavour Fragr. J.* **2010**, *25* (5), 313–326. https://doi.org/10.1002/ffj.2019
49. Yorozu, T.; Hoshino, M.; Imamura, M. *J. Phys. Chem.* ***1982****, 86* (22), 4426-4429. https://doi.org/10.1021/j100219a031
50. Gasbarri, C.; Guernelli, S.; Boncompagni, S.; Angelini, G.; Siani, G.; De Maria, P.; Fontana, A. *J. Liposome Res.* **2010**, *20*, 202–210. https://doi.org/10.3109/08982100903244526
51. Murthy, C. N.; Geckeler, K. E. *Chem Comm.* **2001**, 1194–1195. https://doi.org/10.1039/B102142G
52. Angelini, G.; Cusan, C.; De Maria, P.; Fontana, A.; Maggini, M.; Pierini, M.; Prato, M.; Schergna, S.; Villani, C. *Eur. J. Organic Chem.* **2005**, *9*, 1884-1891. https://doi.org/10.1002/ejoc.200400699
53. Zung, J.; Ndou, N.; Warner, I. *Applied Spectroscopy* **1990**, *44*, 1491-1493. https://doi.org/10.1366/0003702904417823
54. Szejtli J. *Chem Rev.* **1998**, *98* (5), 1743-1754.

https://doi.org/10.1021/cr970022c
55. Rosseels, M.L.; Delaunois, A.G.; Hanon, E.; Guillaume, P.J.; Martin, F.D.; van den Dobbelsteen, D.J. *Regul. Toxicol. Pharmacol.* **2013**, *67*(3), 351-9. https://doi.org/10.1016/j.yrtph.2013.08.013
56. Yokoo, M.; Kubota, Y.; Motoyama, K.; Higashi, T.; Taniyoshi, M.; Tokumaru, H.; Nishiyama, R.; Tabe, Y.; Mochinaga, S.; Sato, A.; Sueoka-Aragane, N.; Sueoka, E.; Arima, H.; Irie, T.; Kimura, S. *PLoS One* **2015**, *10* (11), e0141946. https://doi.org/10.1371/journal.pone.0141946
57. Arima, H.; Yunomae, K.; Morikawa, T.; Hirayama, F.; Uekama, K. *Pharm. Res.* **2004**, *21* (4), 625–634. https://doi.org/10.1023/B:PHAM.0000022409.27896.d4
58. Krait, S.; Salgado, A.;Malanga, M.;Sohajda, T.; Benkovics, G.; Szakály, P.S.; Chankvetadze, B.; Scriba, G.K.E. *J. Chromatogr. A* **2022**, *1661*, 462675. https://doi.org/10.1016/j.chroma.2021.462675
59. Stella, V.J.; Rajewski, R.A. *Int. J. Pharm.* **2020**, *583*, 119396. https://doi.org/10.1016/j.ijpharm.2020.119396
60. Tongiani, S.; Ozeki, T.; Stella, V.J. *J. Pharm. Sci.* **2009**, *98* (12), 4769–4780. https://doi.org/10.1002/jps.21791
61. Kochkar, H.; Aouine, M.; Ghorbel, A.; Berhault, G. *J. Phys. Chem. C.* **2011**, *111*, 11364–11373. https://doi.org/10.1021/jp200662j
62. Gandhi, S.; Shende, P. *J. Control. Release* **2021**, *339*, 41-50. https://doi.org/10.1016/j.jconrel.2021.09.025
63. George, C.; Kuriakose, S.; Prakashkumar, B.; Mathew, T. *Supramol. Chem.* **2010**, *22*, 511–516. https://doi.org/10.1080/10610278.2010.487565
64. Chae, H.H.; Kim, B.H.; Yang, K.S.; Rhee, J.I. *Synth. Met.* **2011**, *161*, 2124–2128. https://doi.org/10.1016/j.synthmet.2011.08.013
65. Andrade, P.F.; de Faria, A.F.; da Silva, D.S.; Bonacin, J.A.; do Carmo Gonçalves, M. *Coll. Surf. B: Biointerfaces* **2014**, *118*, 289–297. https://doi.org/10.1016/j.colsurfb.2014.03.032
66. Pandey, A. *Environ. Chem. Lett.* **2021**, *19*, 4297-4310. https://doi.org/10.1007/s10311-021-01275-y
67. Chen, X.; Parker, S.G.; Zou, G.; Su, W.; Zhang, Q. *ACS Nano* **2010**, *4* (11), 6387–6394. https://doi.org/10.1021/nn1016605
68. Hu, Q.D.; Tang, G.P.; Chu P.K. *Acc. Chem. Res.* **2014**, *47* (7), 2017–2025. https://doi.org/10.1021/ar500055s
69. Suriati, G.; Mariatti, M.; Azizan, A. *Int. J. Automot. Mech. Eng.* **2014**, *10*, 1920-1927. https://doi.org/10.15282/ijame.10.2014.9.0160
70. Quintero-Quiroz, C.; Acevedo, N.; Zapata-Giraldo, J.; Botero, L.E.; Quintero, J.; Zárate-Triviño, D.; Saldarriaga, J.; Pérez, V.Z. *Biomater. Res.* **2019**,*19*, 23-27. https://doi.org/10.1186/s40824-019-0173-y
71. Jaiswal, S.; Duffy, B.; Jaiswal, A.K.; Stobie, N.; McHale, P. *Int. J. Antimicrob. Agents* **2010**, *36*, 280-283. https://doi.org/10.1016/j.ijantimicag.2010.05.006
72. Priya, R.S.; Geetha, D.; Ramesh, P.S. *Carbon Sci. Technol.* **2013**, *1*, 197-202.
73. Amiri, S.; Duroux, L.; Larsen, K. L. *J. Nanopart. Res.* **2015**, *17*, 21-38. https://doi.org/10.1007/s11051-014-2820-5

74. Suárez-Cerda, J.; Nuñez, G.A.; Espinoza-Gómez, H.; Flores-López, L.Z. *Mat. Science Eng. C* **2014**, *43*, 21–26. https://doi.org/10.1016/j.msec.2014.07.006
75. Kochkar, H.; Aouine, M.; Ghorbel, A.; Berhault, G. *J. Phys. Chem. C* **2011**, *115*, 11364–11373. https://doi.org/10.1021/jp200662j
76. Rajamanikandan, R.; Ilanchelian, M. *Mat. Today Comm.* **2018**, *15*, 61-69. https://doi.org/10.1016/j.mtcomm.2018.02.024
77. Yang, L.; Chen, Y.; Li, H.; Luo, L.; Zhao, Y.; Zhang, H.; Tian, Y. *Anal. Methods* **2015**, *7* (16), 6520–6527. https://doi.org/10.1039/C5AY01212K
78. Ventimiglia, G.; Motta, A. *Sens. Transducers. J.* **2012**, *146*, 59-68.
79. Pande, S.; Ghosh, S. K.; Praharaj, S.; Panigrahi, S.; Basu, S.; Jana, S.; Pal, A.; Tsukuda T.; Pal, T. *J. Phys. Chem. C* **2007**, *111*, 10806-10813. https://doi.org/10.1021/jp0702393
80. Li, P.; Li, S.; Wang, Y.; Zhang, Y.; Han, G.Z. *Coll. Surfaces A: Physicochem. Eng. Aspects* **2017**, *520*, 26-31. https://doi.org/10.1016/j.colsurfa.2017.01.034
81. Angelini, G.; Gasbarri, C., *Coll. Surfaces A: Physicochem. Eng. Aspects* **2022**, *633*, 127924. https://doi.org/10.1016/j.colsurfa.2021.127924
82. Premkumar, T.; Geckeler, K.E. *New J. Chem.* **2014**, *38*, 2847-2855. https://doi.org/10.1039/c3nj01375h
83. Jiang, Y.; Sun, D.W.; Pu, H.; Wei, Q. *Talanta* **2019**, *197*, 151–158. https://doi.org/10.1016/j.talanta.2019.01.015
84. Liu, C.; Feng, X.; Qian, H.; Fang, G.; Wang, S. *Food Anal. Methods* **2015**, *8* (3), 596–603. https://doi.org/10.1007/s12161-014-9936-1
85. Chen, Y.; Li, X.; Yang, M.; Yang, L.; Han, X.; Jiang, X.; Zhao, B. *Talanta* **2017**, *167*, 236–241. https://doi.org/10.1016/j.talanta.2017.02.022
86. Qiu, X. Gu, J.; Yang, T.; Ma, C.; Li, L.; Wu, Y.; Zhu, C.; Gao, H.; Yang, Z.; Wang, Z.; Li, X.; Hu, A.; Xu, J.; Zhong, L.; Shen, J.; Huang, A.; Chen, G. *Spectrochim. Acta Part A: Mol. Biomol. Spectrosc.* **2022**, *276*, 121212. https://doi.org/10.1016/j.saa.2022.121212
87. Maia, P. P.; de Sousa, S. M. R.; De Almeida, W. B.; Guimarães, L.; Nascimento Jr., C.S. *J. Mol. Model* **2016**, *22*, 220. https://doi.org/10.1007/s00894-016-3098-6
88. De Maria, P.; Fontana, A.; Siani, G.; D'Aurizio, E.; Cerichelli, G.; Chiarini, M.; Angelini, G.; Gasbarri, C., *Colloids Surf. B: Biointerfaces* **2011**, *87*, 73–78. https://doi.org/10.1016/j.colsurfb.2011.05.003
89. Mishra, A.; Dheepika, R.; Parvathy, P.A.; Imram, P.M.; Bhuvanesh, N.S.P.; Nagarajan, S. *Sci. Rep.* **2021**, *11*, 19324. https://doi.org/10.1038/s41598-021-97832-0
90. Angelini, G.; Campestre, C.; Boncompagni, S.; Gasbarri, C. *Chem. Phys. Lipids* **2017**, *209*, 61-65. https://doi.org/10.1016/j.chemphyslip.2017.09.004
91. Kavitha, S.R.; Umadevi, M.; Vanelle, P.; Terme, T.; Khoumeri, O.; Sridhar, B. *Spectrochim. Acta Part A Mol. Biomol. Spectrosc.* **2014**, *133*, 472–479. https://doi.org/10.1016/j.saa.2014.06.007
92. Donoso-González, O.; Lodeiro, L.; Aliaga, Á.E.; Laguna-Bercero, M.A.; Bollo, S.; Kogan, M.J.; Yutronic, N.; Sierpe, R. *Pharmaceutics* **2021**, *13* (2), 261. https://doi.org/10.3390/pharmaceutics13020261

93. Liu, C.; Lian, J.; Liu, Q.; Xu, C.; Li, B. *Anal. Methods* **2016**, *8*, 5794-5800. https://doi.org/10.1039/C6AY01308B
94. Dhavle, V.; Kateshiya, M.R.; Park, TJ.; Kailasa, S.K. *J. Electron. Mater.* **2021**, *50*, 3676–3685. https://doi.org/10.1007/s11664-021-08875-y
95. Wu, J.; Ma, H. Bu, X.; Ma, C.; Zhu, L.; Hao, B.; Zhao, B.; Tian, Y. *Microchimica Acta* **2019**, *186*, 801. https://doi.org/10.1007/s00604-019-3946-z
96. Schatz, G.C. *Acc. Chem. Res.* **1984**, *17* (10), 370–376. https://doi.org/10.1021/ar00106a005
97. Song, Z.; Wu, Y.; Wang, H.; Han, H. *Mater. Sci. Eng. C* **2019**, *99*, 255-263. https://doi.org/10.1016/j.msec.2018.12.053
98. Khan, M.J.; Shameli, K.; Sazili, A.Q.; Selamat, J.; Kumari, S. *Molecules* **2019**, *24*, 719. https://doi.org/10.3390/molecules24040719
99. Yang, X.X.; Li, C.M.; Huang, C.Z. *Nanoscale* **2016**, *8*, 3040-3048. https://doi.org/10.1039/C5NR07918G
100. Jahed, V.; Zarrabi, A.; Bordbar, A.; Hafezi, M.S. *Food Chemistry* **2014**, *165*, 241-246. https://doi.org/10.1016/j.foodchem.2014.05.094
101. Gupta, A.; Briffa, S.M.; Swingler, S.; Gibson, H.; Kannappan, V.; Adamus, G.; Kowalczuk, M.; Martin, C.; Radecka, I. *Biomacromolecules* **2020**, *21*, 1802-1811. https://doi.org/10.1021/acs.biomac.9b01724
102. Alsammarraie, F.K.; wang, W.; Zhou, P.; Mustapha, A.; Lin, M. *Colloids Surf. B* **2018**, *171*, 398-405. https://doi.org/10.1016/j.colsurfb.2018.07.059
103. Srivatsan, K.V.; Duraipandy, N.; Begum, S.; Lakra, R.; Ramamurthy, U.; Korrapati, P.S.; Kiran, M.S. *Int. J. Biol. Macromol.* **2015**, *75*, 306-315. https://doi.org/10.1016/j.ijbiomac.2015.01.050
104. Chadha, R.; Das, A.; Lobo, J.; Meenu, V.O.; Paul, A.; Ballal, A.; Maiti, N. *Coll. Surfaces A: Physicochem. Eng. Aspects* **2022**, *641*, 128558. https://doi.org/10.1016/j.colsurfa.2022.128558
105. Ganesan, V.; Senguttuvan, S.; Narayanan, V.; Shanmugasundaran, E.; Vellaisamy, K.; Varadharajan,R.; Duraisamy, R.; Govindasamy, M.; Thambusamy, S. *Chem. Phys. Letters* **2022**, *796*, 139537. https://doi.org/10.1016/j.cplett.2022.139537
106. Hoyos-Palacio, L.M.; Cuesta Castro, D.P.; Ortiz-Trujillo, I.C.; Botero Palacio, L.E.; Galeano Upegui, B.J.; Escobar Mora, N.J.; Carlos Cornelio, J.A. *J. Mater. Res. Technol.* **2019**, *8* (6), 5893–5898. https://doi.org/10.1016/j.jmrt.2019.09.062
107. Hui, B.Y.; Zain, N.N.M.; Mohamad, S.; Prabu, S.; Osman, H.; Raoov, M. *J. Mol. Struct.* **2020**, *1206*, 127675. https://doi.org/10.1016/j.molstruc.2019.127675
108. Gannimani, R.; Ramesh, M.; Mtambo, S.; Pillay, K.; Soliman, M.E.; Govender, P. *J. Inorg. Biochem.* **2016**, *157*, 15–24. https://doi.org/10.1016/j.jinorgbio.2016.01.008
109. Moskovits, M.; Suh, J. *J. Am. Chem. Soc.* **1985**, *107*, 6826-6829. https://doi/10.1021/ja00310a014
110. Leyton, P.; Domingo, C.; Sanchez-Cortes, S.; Campos-Vallette, M.; Garcia-Ramos, J. *Langmuir* **2005**, *21*, 11814-11820. https://doi.org/10.1021/la051761o
111. Ng, C. H. B.; Yang, J.; Fan, W.Y. *J. Phys. Chem. C* **2008**, *112*, 4141-4145.

https://doi.org/10.1021/jp710553c
112. Yuan, Y.; Zhang, F.; Wang, Y.; Li, X.; Zhao, R.; Shao, D.; Bi, S. *Microchemical J.* **2022**, *172*, 106938. https://doi.org/10.1016/j.microc.2021.106938
113. Tarakeshwar, P.; Finkelstein-Shapiro, D.; Hurst, S.J.; Rajh, T.; Mujica, V. *J. Phys. Chem. C* **2011**, *115* (18), 8994–9004. https://doi.org/10.1021/jp202590e
114. Wang, M.; Wang, J.; Wang, Y.; Liu, C.; Liu, J.; Qiu, Z.; Xu, Y.; Lincoln, S.F.; Guo, X. *Colloid Polym. Sci.* **2016**, *294*, 1087–95. https://doi.org/10.1007/s00396-016-3867-x
115. Wang, Y.; Feng, Z.; Sun, Y.; Zhu, L.; Xia, D. *Soft Matter* **2022**, *18*, 975-982. https://doi.org/10.1039/D1SM01248G
116. Wang, Y.; Sun, Y.; Bian, H.; Zhu, L.; Xia, D.; Wang, H. *ACS Appl. Mater. Interfaces* **2020**, *12*, 45916-45928. https://doi.org/10.1021/acsami.0c15836
117. Koczkur, K.M.; Mourdikoudis, S.; Polavarapu, L.; Skrabalak, S.E. *Dalton Trans.* **2015**, *44*, 17883-17905. https://doi.org/10.1039/C5DT02964C
118. Wang, Y.; Chen, Y.; Bian, H.; Sun, Y.; Zhu, L.; Xia, D. *Sens. Actuators B* **2021**, *341*, 130044. https://doi.org/10.1016/j.snb.2021.130044
119. Siewdorlang, D.; Negi, D.P.S. *Spectrochim. Acta Part A* **2019**, *215*, 203-208. https://doi.org/10.1016/j.saa.2019.02.101
120. Qin, L.; Xie, F.; Jin, X.; Liu, M. *Chem. Eur. J.* **2015**, *21*, 11300-11305. https://doi.org/10.1002/chem.201500929

Authors' Biographies

Carla Gasbarri is Assistant Professor of Organic Chemistry at the University « G. d'Annunzio » of Chieti-Pescara where she received her Ph.D. in Pharmaceutical Sciences in 2004. Her main research topics are the synthesis and characterization of silver nanoparticles and their interactions with natural and bioactive compounds; energetic, kinetic and thermodynamic investigation of cis-trans isomerization, keto-enol tautomerism and reversible reactions in organic solvents and non-conventional media; preparation of supramolecular aggregates as liposomes, micelles and host-guest inclusion complexes for potential applications in delivery systems.

Guido Angelini received his Ph.D. in Pharmaceutical Sciences at the University "G. d'Annunzio" of Chieti-Pescara in 2002. The thesis topic was: "Study of supramolecular aggregates of amphiphilic molecules." After post-doctoral studies on the inclusion of organic molecules in liposomes formed by natural and synthetic surfactants, he joined the Faculty of Pharmacy in 2006 as Assistant Professor of Organic Chemistry. His research interests include microwave synthesis of organic compounds and interactions studies by Isothermal Titration Calorimetry; preparation of metal nanoparticles; thermodynamic and kinetic study of keto-enol tautomerism of alfa-nitroketones in aprotic solvents and in ionic liquids.